

Synthesis and Optical Properties of $\text{CaY}_2\text{Al}_4\text{SiO}_{12}:\text{Ce}^{3+}$

Arturas Katelnikovas^{a,b}, Holger Winkler^c, Aivaras Kareiva^b, Thomas Jüstel^a



^aDepartment of Chemical Engineering, Münster University of Applied Sciences, Steinfurt, Germany

^bDepartment of General and Inorganic Chemistry, Vilnius University, Vilnius, Lithuania

^cMerck KGaA, Darmstadt, Germany



Introduction

The most widely applied phosphor in white LEDs is cerium doped yttrium aluminum garnet (YAG:Ce). It shows strong absorption in the blue and broad emission band in the yellow spectral region. The position of the Ce^{3+} emission band depends on crystal-field strength, covalency and Stokes shift. It is known that substitution of Y at dodecahedral sites by larger cations results in a red shift of emission, whereas smaller cations causes a blue shift. The opposite result is observed for octahedral and tetrahedral sites. The larger cation introduced into octahedral or tetrahedral site leads to a blue shift of emission and a smaller one a red shift. Another option for a blue or red shift of YAG:Ce emission band is substitution of yttrium by divalent or tetravalent cation, respectively. However, it is quite hard to find a large enough tetravalent cation for the voluminous dodecahedral sites. On the other hand, there are plenty of divalent cations suitable for substitution of yttrium. We show that substitution of Y^{3+} by Ca^{2+} leads to a blue shift of the Ce^{3+} emission band. The present finding can be explained by reduction of crystal-field strength due to a decrease of effective charge of dodecahedral site.

Synthesis

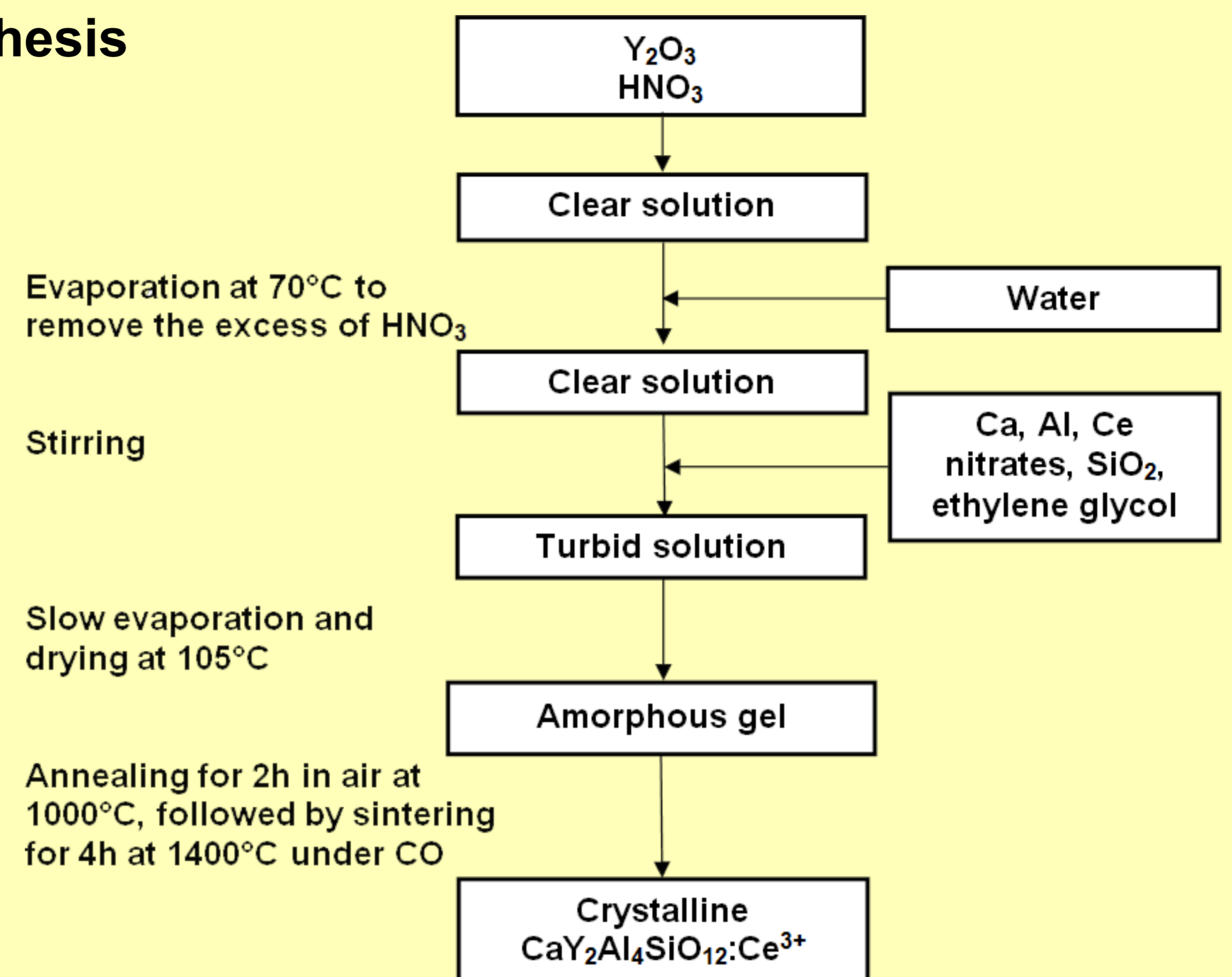


Fig.1. Scheme of the sol-gel synthesis procedure of $\text{CaY}_2\text{Al}_4\text{SiO}_{12}:\text{Ce}^{3+}$ samples

Results and Discussion

All samples were synthesized by a sol-gel method employing ethylene glycol as a chelating agent. The complete synthesis procedure is shown in Fig. 1. It turned out that sintering powders at 1400 C resulted in single-phase garnet materials (see Fig. 2). Phosphors possessed a green to yellow body color indicating the absorption in the blue what is in line with the reflection spectra represented in Fig. 3. As expected the absorption in the blue increased with higher Ce^{3+} concentration. However, higher Ce^{3+} amounts have led to greyish samples probably due to defect formation. Excitation and emission spectra are depicted in Fig. 4. The maximum excitation and emission intensity was achieved if phosphors were doped by 1% Ce^{3+} .

Further increase of dopant concentration led to a decrease of intensity and a red shift of emission maximum due to re-absorption of emitted photons by the activator. Fig. 5 shows the thermal quenching of the sample doped by 0.5% Ce^{3+} . It reveals that emission intensity decreases if temperature is increased. Boltzmann method was employed to calculate $\text{TQ}_{1/2}$ value ($\text{TQ}_{1/2}$ indicates the temperature at which the phosphor loses 50% of its quantum efficiency). It turned out that pending phosphor loses half of efficiency at 458 K (≈ 185 C). Color points of synthesized phosphors are shown in Fig. 6. It is obvious that the increase of Ce^{3+} concentration leads to a red-shift of the color point towards YAG:Ce, which is in line with emission spectra. Finally, quantum efficiencies were calculated and are presented in Fig. 7.

It turned out that QE gradually decreased if Ce^{3+} concentration was increased. However, QE is still too low for application in pcLEDs, but it could be improved by Ce^{3+} concentration and particle size, shape optimization..

Conclusions

In this work we demonstrated that the reduction of effective charge of dodecahedral site in YAG has led to decrease of crystal-field strength. As a consequence the emission maximum of Ce^{3+} shifted towards green spectral region (≈ 550 nm) compared with conventional YAG:Ce emitting at 560 nm.

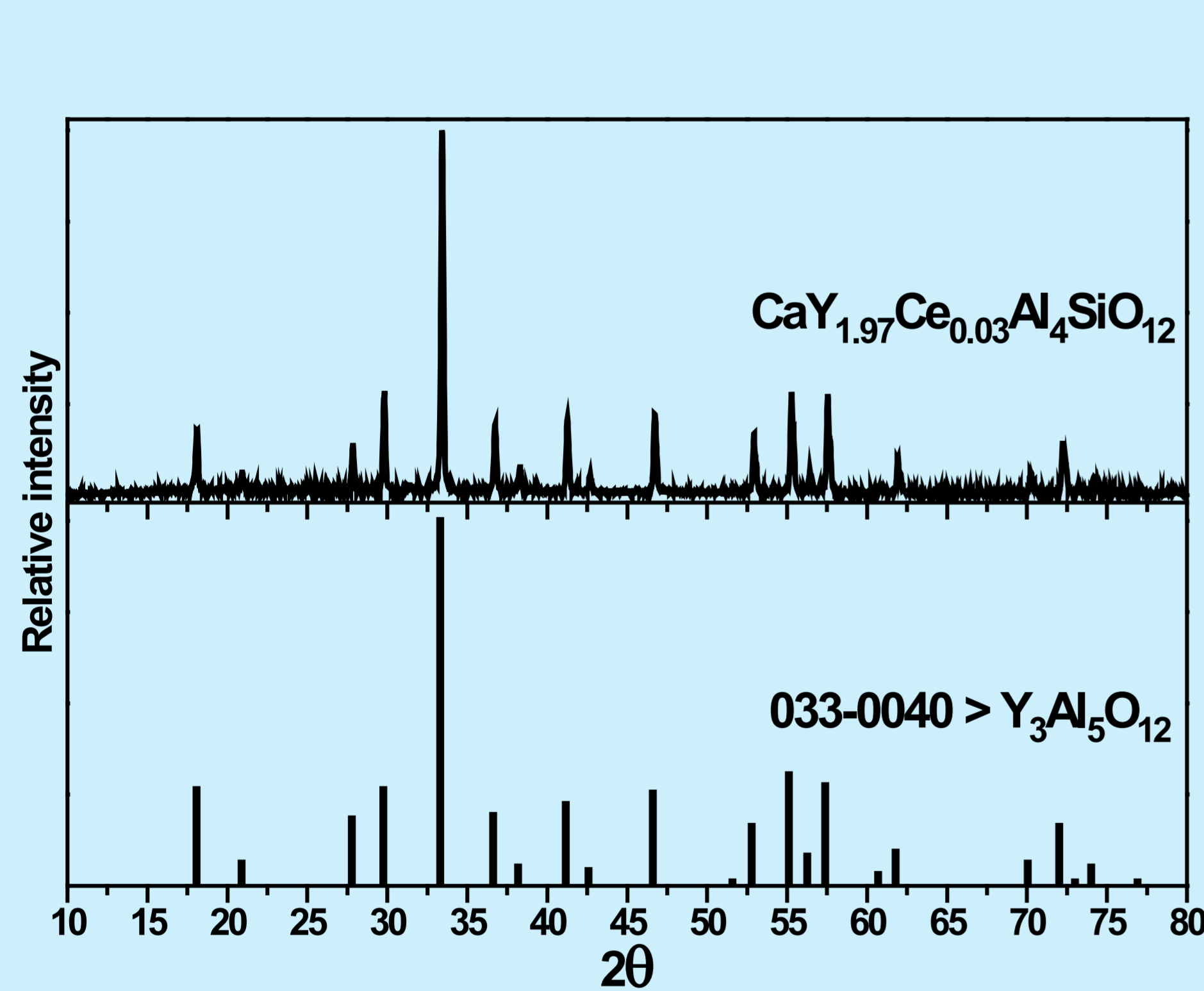


Fig. 2. XRD pattern of $\text{CaY}_{1.97}\text{Ce}_{0.03}\text{Al}_4\text{SiO}_{12}$

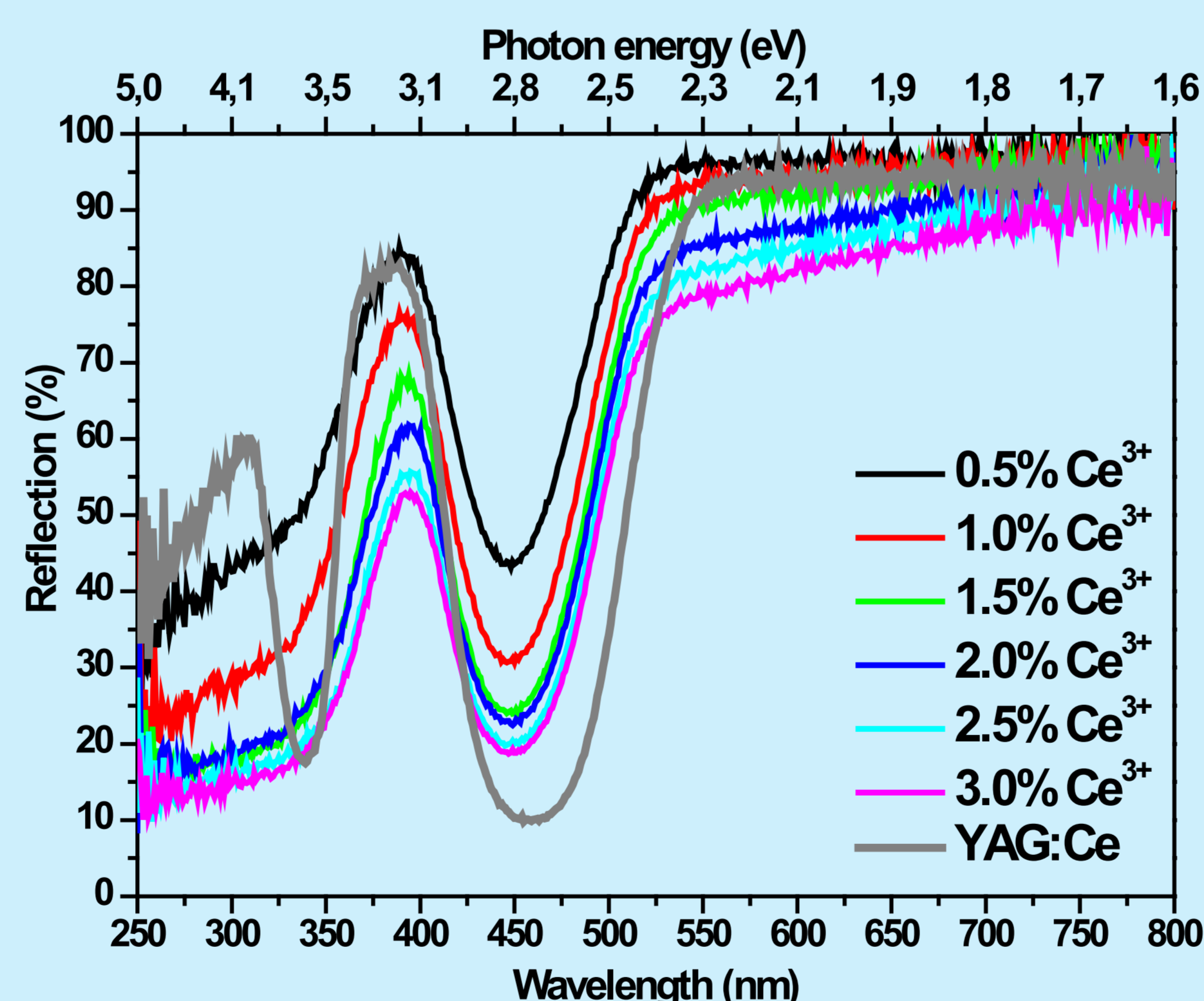


Fig. 3. Reflection spectra of $\text{CaY}_2\text{Al}_4\text{SiO}_{12}:\text{Ce}^{3+}$ samples

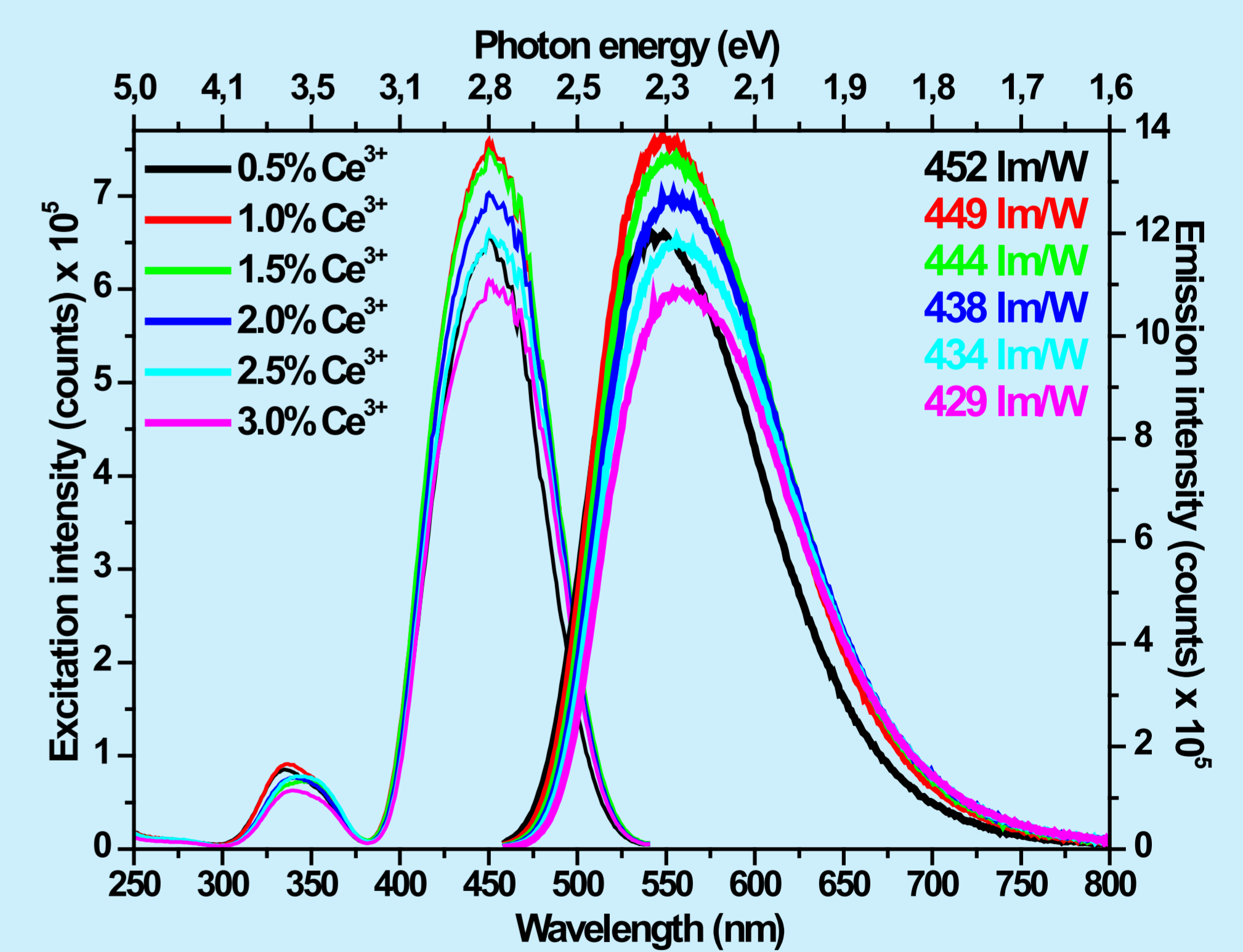


Fig. 4. Excitation and emission spectra of $\text{CaY}_2\text{Al}_4\text{SiO}_{12}:\text{Ce}^{3+}$ samples and their lumen equivalents

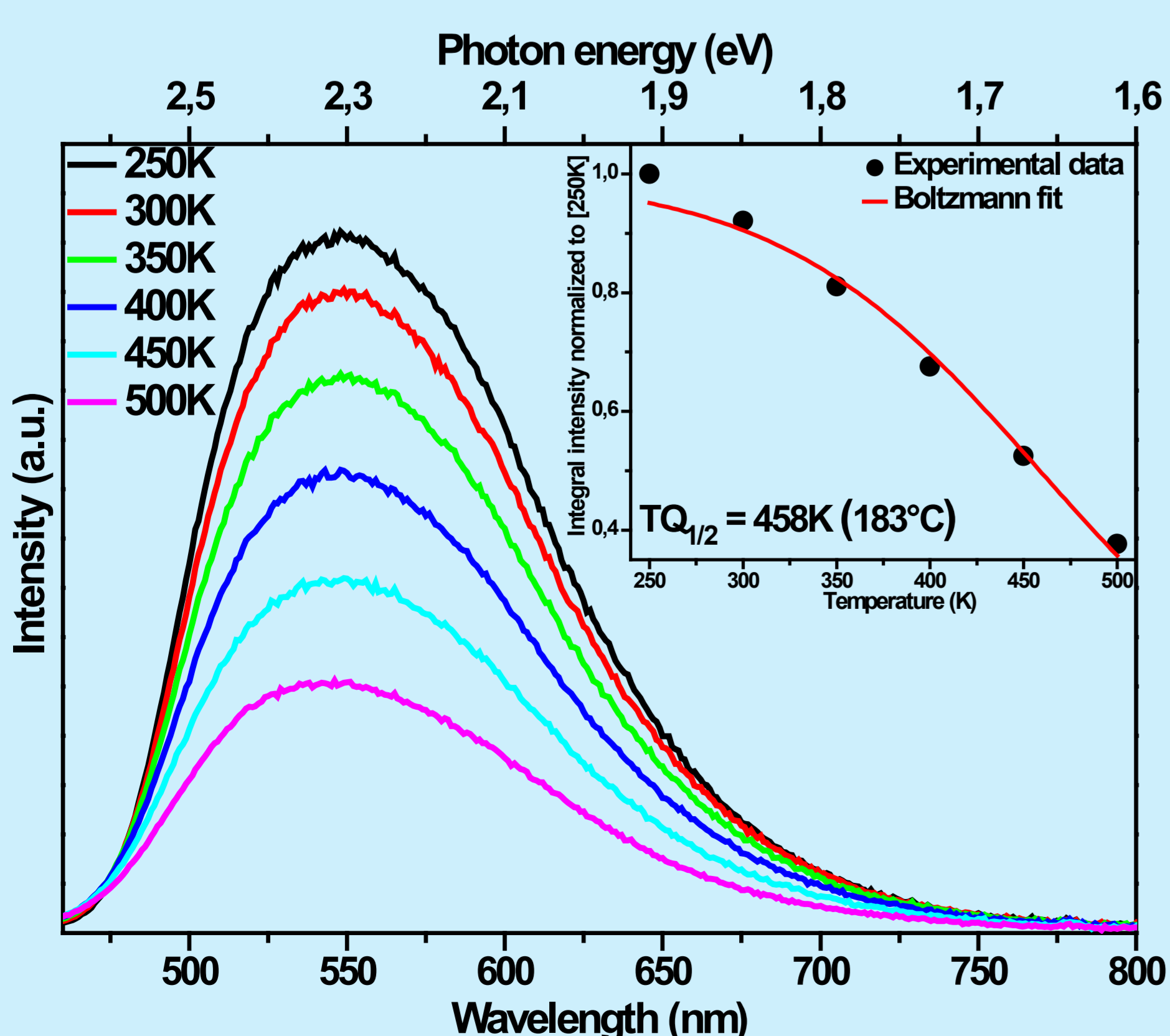


Fig. 5. Temperature dependent emission spectra of $\text{CaY}_{1.985}\text{Ce}_{0.015}\text{Al}_4\text{SiO}_{12}$

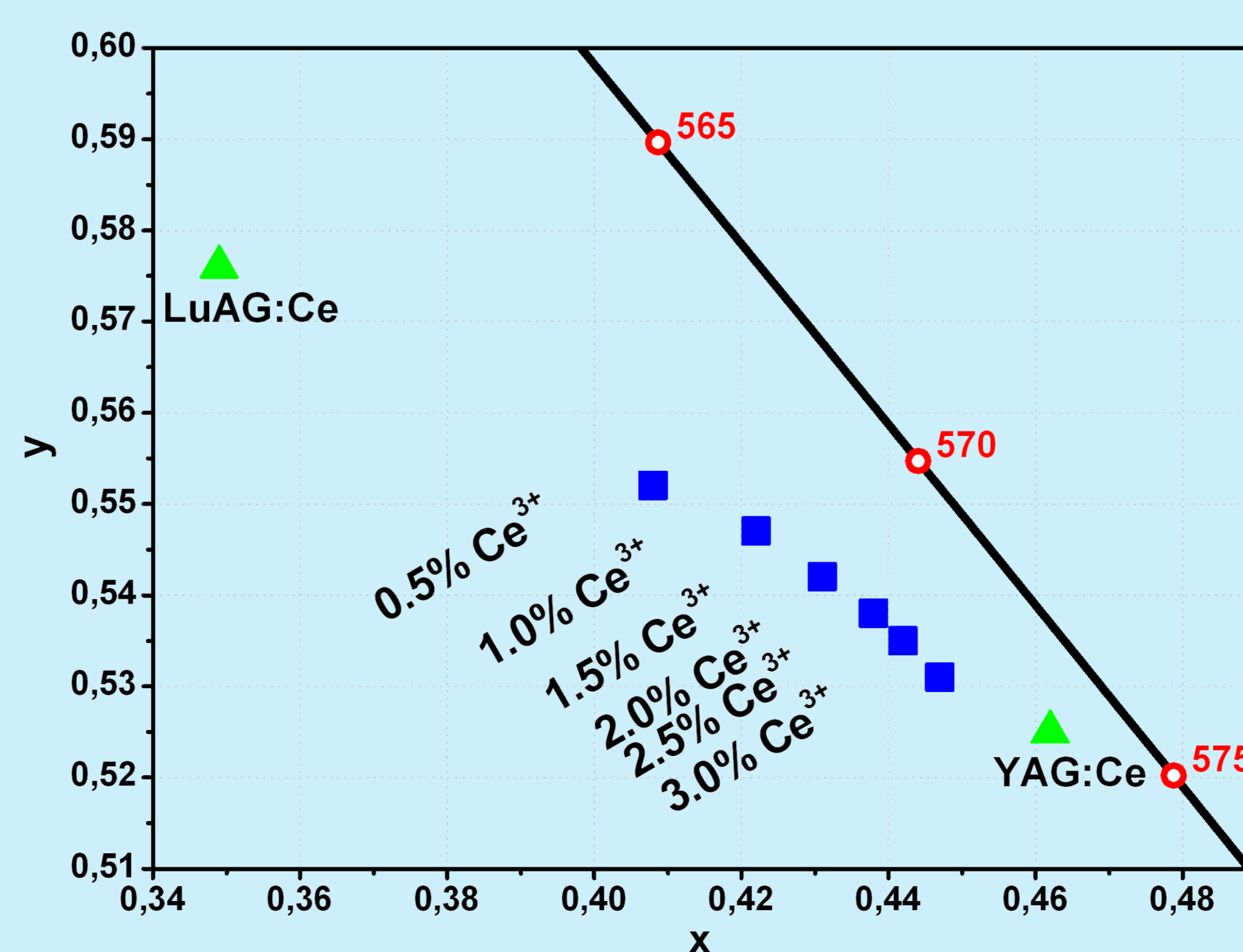


Fig. 6. CIE 1931 color points of $\text{CaY}_2\text{Al}_4\text{SiO}_{12}:\text{Ce}^{3+}$ as function of the Ce^{3+} concentration

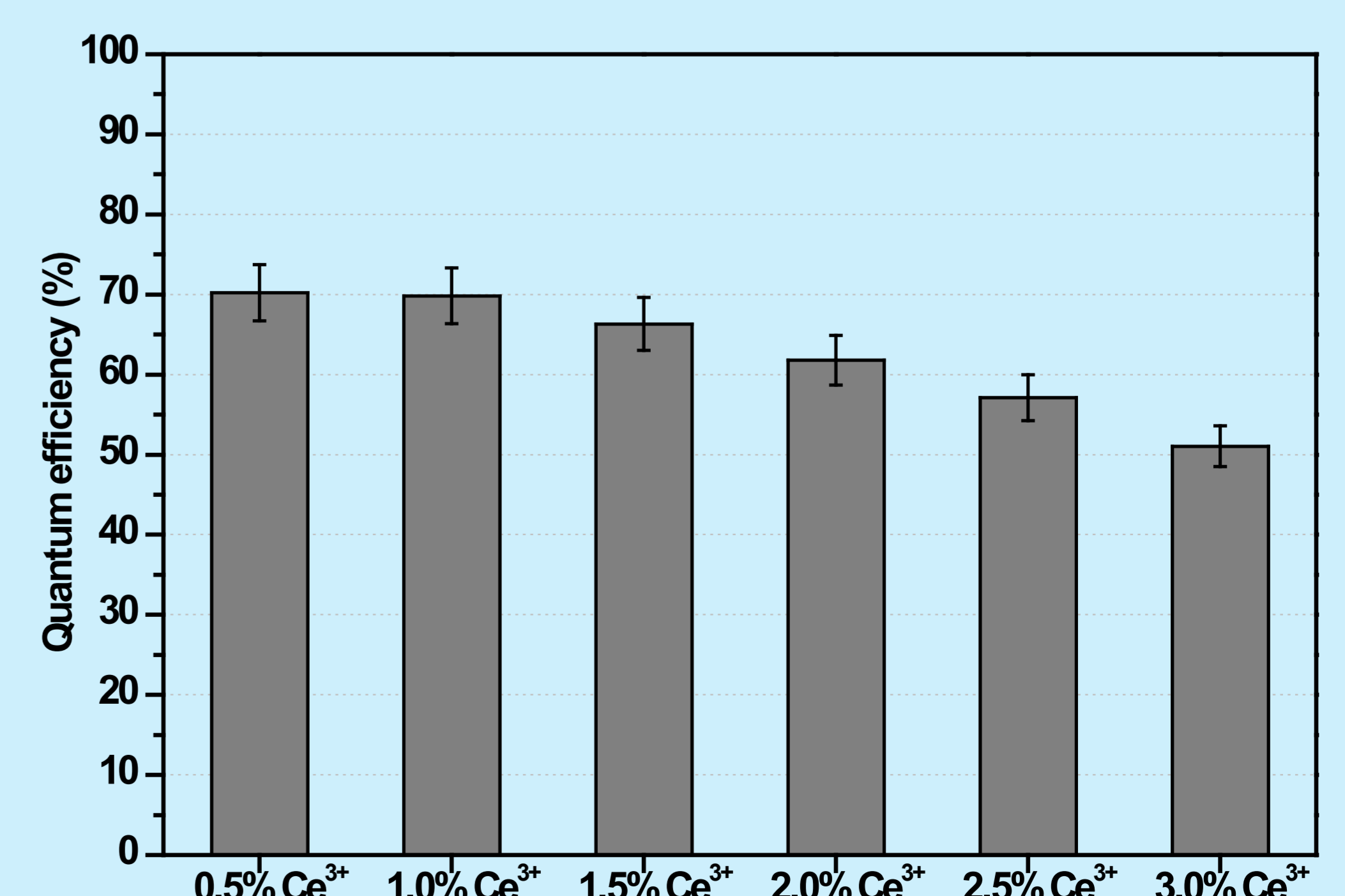


Fig. 7. Quantum efficiencies of $\text{CaY}_2\text{Al}_4\text{SiO}_{12}:\text{Ce}^{3+}$ samples